Journal of Hazardous Materials 477 (2024) 135244

Contents lists available at ScienceDirect

Journal of Hazardous Materials

journal homepage: www.elsevier.com/locate/jhazmat

Water-fertilizer regulation drives microorganisms to promote iron, nitrogen and manganese cycling: A solution for arsenic and cadmium pollution in paddy soils

Ting Zhang [a,b,1], Yifei Sun [a,1], Sanjai J. Parikh [c], Gilles Colinet [b], Gina Garland [d], Lijuan Huo [e], Nan Zhang [a], Hong Shan [a], Xibai Zeng [a], Shiming Su [a,*]

[a] Institute of Environment and Sustainable Development in Agriculture, Chinese Academy of Agricultural Sciences/Key Laboratory of Agro-Environment, Ministry of Agriculture, Beijing 100081, China
[b] TERRA Teaching and Research Centre, Gembloux Agro-Bio Tech, University of Liege, Gembloux 5030, Belgium
[c] Department of Land, Air and Water Resources, University of California Davis, Davis, CA 95616, USA
[d] Department of Environmental System Science, ETH Zurich, Zurich 8046, Switzerland
[e] School of Environment and Resources, Taiyuan University of Science and Technology, Waliu Road No 66, Taiyuan 030024, China

HIGHLIGHTS

- Applying biochar or CMP fertilizer in aerobic soil mitigate Cd and As simultaneously.
- Moisture or fertilizer affects the onset conditions of key element redox cycles.
- In drained soil, Fe, Mn, N redox are key cycles to reduce Cd and As bioavailability.
- The nitrification and Mn transport gene abundance increase in aerobic soils.
- Functional gene abundance was regulated by microbial community composition.

GRAPHICAL ABSTRACT

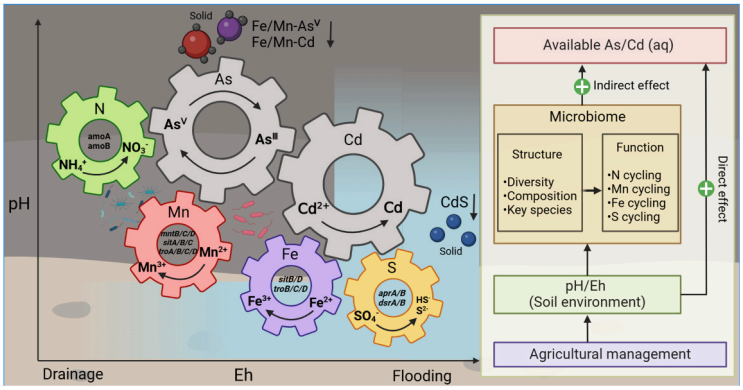

ARTICLE INFO

Keywords:
Arsenic
Cadmium
Water regime
Fertilizer regime
Microbial process

ABSTRACT

The co-contamination of arsenic (As) and cadmium (Cd) in rice fields presents a global imperative for resolution. However, understanding the complex microbially driven geochemical processes and network connectivity crucial for As and Cd bioavailability under the frequent redox transitions in rice fields remains limited. Here, we conducted a series of microcosm experiments, using flooding and drainage, alongside fertilization treatments to emulate different redox environment in paddy soils. Soil As significantly reduced in drained conditions following applications of biochar or calcium-magnesium-phosphate (CMP) fertilizers by 26.3 % and 31.2 %, respectively, with concurrent decreases in Cd levels. Utilizing geochemical models, we identified the primary redox cycles

* Correspondence to: Institute of Environment and Sustainable Development in Agriculture, Chinese Academy of Agricultural Sciences, Zhongguancun South Street No 12, Beijing 100081, China.
E-mail address: sushiming@caas.cn (S. Su).
[1] These authors contributed equally to this work and share first authorship.

https://doi.org/10.1016/j.jhazmat.2024.135244
Received 12 April 2024; Received in revised form 10 July 2024; Accepted 16 July 2024
Available online 17 July 2024

dynamically altering during flooding (Fe and S cycles) and drainage (Fe, Mn, and N cycles). PLS-SEM elucidated 76 % and 61 % of the variation in Cd and As through Mn and N cycles. Functional genes implicated in multi-element cycles were analyzed, revealing a significantly higher abundance of assimilatory N reduction genes (*nasA, nirA/B, narB*) in drained soil, whereas an increase in ammonia-oxidizing genes (*amoA/B*) and a decrease in nitrate reduction to ammonium genes were observed after CMP fertilizer application. Biochar application led to significant enrichment of the substrate-binding protein of the Mn transport gene (*mntC*). Moreover, Fe transport genes were enriched after biochar or CMP application compared to drained soils. Among 40 high-quality metagenome-assembled genomes (MAGs), microbial predictors associated with low Cd and As contents across different treatments were examined. Bradyrhizobacea harbored abundant Mn and Fe^{III} transport genes, while Nitrososphaeraceae carried nitrification-related genes. Two MAGs affiliated with Caulobacteraceae, carrying diverse Fe transport genes, were enriched in biochar-applied soils. Therefore, applying CMP fertilizer or biochar in aerobic rice fields can synergistically reduce the bioavailability of Cd and As by specifically enhancing the circulation of essential elements.

1. Introduction

Due to both natural geological processes and anthropogenic activities such as mining and smelting, the co-occurrence of cadmium (Cd) and arsenic (As) in global farmland is widespread [1,2]. These compounds, classified as Group I human carcinogens [3], are known to pose serious threats to human health through the food chain [4]. In paddy fields, the competent accumulation of Cd and As in rice can lead to various diseases, including itai-itai disease and cardiovascular diseases [5]. Under anoxic conditions, Cd primarily exists as CdS, an insoluble compound with low bioavailability [6], while As exists in the form of cytotoxic inorganic As (iAs) oxides such as arsenite (As^{III}) and arsenate (As^{V}), as well as relatively less toxic phytotoxic organoarsenic oxides (oAs) such as dimethylarsenic (DMA) [7,8]. Arsenic is most soluble under reducing conditions (anoxic), primarily as As^{III}, whereas Cd is most soluble in oxidizing conditions (oxic) as $CdSO_4$ [9]. These opposing geochemical properties present challenges in efficiently managing Cd and As bioavailability in paddy soils. Therefore, urgent attention is needed to develop effective methods to synergistically remediate farmlands co-contaminated with Cd and As, as well as to elucidate the critical mechanisms for reducing Cd and As bioavailability.

Arsenic and Cd cycling in soil is coupled with the redox cycles of nitrogen (N), iron (Fe), manganese (Mn), sulfur (S) and other elements, which further affect their solubility, toxicity and bioavailability [10,11]. Moreover, these processes are impacted by soil moisture, mediated in paddy soils by flooding and drainage, due to the different redox potentials (Eh) and pH values these processes facilitate [9,12]. When paddy fields are flooded, the reductive dissolution of Fe and Mn (hydr) oxides and the reduction of As^{V} results in an increase in As^{III} mobility and bioavailability [13]. Upon drainage, Cd is mobilized from Fe/Mn-(hydr) oxides resulting in a substantial dissolution into soil porewater [14]. With sulfate reduction, Cd precipitates as CdS [15]. Arsenite can also co-precipitate or adsorb with sulfides (S^{2-}) [16]. Additionally, the formation of inorganic thioarsenates and methylthioarsenates may also be facilitated by sulfate reduction [17,18]. Furthermore, both ammonium oxidation and nitrate reduction are coupled with As redox reactions, closely intertwined with Fe redox reactions [19,20]. When NO_3^- is reduced to NH_4^+, the bioavailability of Cd in the soil decreases under the influence of microbial activity [21]. Due to the difference in the thermodynamics of electron acceptors, the onset of the redox reactions of each element is different. These intricately coupled chemical cycles profoundly affect the bioavailability of As and Cd in heterogeneous soil systems. In rice fields, regular flooding and draining are essential to ensure yields, as well as the application of organic and chemical fertilizers. During the late tillering stage of rice growth, drainage is performed to promote effective tillering, and then chemical fertilizers are applied to provide nutrients for later jointing and heading. The changes of soil moisture and the increased ion concentration brought by the fertilizers would both be involved in regulating the bioavailability of Cd and As [22,23]. Moreover, fertilization in drained co-contaminated rice fields can effectively and synergistically reduce the availability of Cd and As [24]. Frequent redox transitions make the biogeochemical cycles of elements in the rice field systems very active [25]. However, there is still a lack of comprehensive understanding of its potential link with As and Cd availability in this system.

The soil microbiome plays a critical role in soil ecosystem services, especially in nutrient cycling and biogeochemical processes [26,27]. Microbial communities in paddy soils is profoundly influenced by moisture regulation and the application of both organic and chemical fertilizers [28,29]. However, compared with taxonomy-based approaches, the assemblage of functional genes is considered to provide a better reflection of the functional response of microbial communities to environment factors [30], enabling a deeper understanding of the factors influencing elemental cycles [31]. Interspecific interactions among functional microorganisms in rice fields contribute to potential coupling in the biogeochemical cycles of N, Fe, Mn, S, Cd, and As [17,32-34]. Nonetheless, our comprehension of microbial-driven element cycling in rice fields under temporal dynamics remains limited, and there exist knowledge gaps regarding the specific ecological roles of key indigenous soil microbes and their metabolic potentials associated with elements cycling.

In this study, we conducted a series of microcosm experiments to simulate various soil Eh and pH conditions under typical rice production moisture management and incorporating organic and chemical soil amendments. In situ soil conditioners such as biochar [35] and calcium magnesium phosphate fertilizers [36] are commonly used acidic amendments that effectively regulate the bioavailability of soil Cd and As. These amendments were selected to represent both organic and chemical fertilizers. We hypothesize that a new redox state of soil is formed under the regulation of water and fertilizer, whereby the oxidation of N, Fe, Mn, or the reduction of S, might serve as critical regulatory hubs for reducing the bioavailability of As and Cd. Additionally, microbial activity is proposed to be the primary driving force behind these processes. The objectives of this study were to (1) assess the impact of modulating multi-element cycling networks on mitigating Cd and As bioavailability in soils; and (2) identify the potential key microbiota and functional genes involved in the key biochemical processes under different fertilization regimes. With this information elucidated, we anticipate that this study can provide the groundwork to develop a feasible strategy for the remediation of polymetallic co-pollution in the future.

2. Materials and methods

2.1. Soil sampling and physicochemical characterization

Paddy soil was collected from five different areas within one established paddy field (half a century old), located around the Shimen realgar mine (Fig. S1). The soil primarily originates from the Quaternary red clay parent rock. The surrounding field has an As and Cd content of approximately 66.5 mg kg^{-1} and 0.41 mg kg^{-1} respectively, rendering

the soil in this region an ideal natural laboratory for studying the interaction of natural microbiota and major element cycles with As and Cd co-contamination [24]. Prior to incubation, selected soil properties were measured on air-dried and sieved (<2 mm) soil samples. These properties include pH, organic carbon content, total Cd/As content, as well as available P, K, Mn and Fe contents, which were analyzed using standard methods described previously [12].

2.2. Soil incubation experiments

Indoor soil incubation experiments were conducted to simulate flooded paddy soil (CK), aerobic paddy soil (R), and applying biochar (RB, organic) or calcium-magnesium-phosphate fertilizer (RF, inorganic) in aerobic paddy soil. Each treatment was replicated three times at 3 sampling time points. The Cd and As contents of the selected commercial rice straw biochar and calcium-magnesium-phosphorus fertilizer (with P_2O_5 content greater than 12 %) were found to be lower than the detection limit. For the incubation, 60 g of paddy soil contaminated with both Cd and As, with a pH of 5.17, was added into 100 mL serum bottles covered with aluminum foil. Deionized water was added at 75 % and 35 % ($w_{water}/w_{dry\text{-}soil}$) to simulate flooded and aerobic conditions, respectively, mimicking field conditions. Weigh the bottles every two days to ensure that the soil moisture content is constant at 75 % and 35 %. One week prior to the experiment, the soil and materials were mixed evenly, and the application rates (by weight) of materials were equivalent to local agricultural practices, specifically 1 % biochar (Beijing PhD Union Academy of Agriculture, Beijing, China) and 0.5 ‰P of calcium-magnesium-phosphate fertilizer (Phosphate Fertilizer Factory in Liuyang East District, Liuyang, China). All samples were then incubated in the dark in a climate chamber at 37 ℃ for 40 days to simulate the single moisture condition of rice from transplanting to the heading stage.

2.3. Soil sampling and chemical analysis

Subsamples were collected on days 1, 20, and 40 of the incubation period. In-situ pH and Eh were tested before sampling, and soil solution was extracted as previously described [24]. The available concentrations of As and Cd were extracted with 1 M KH_2PO_4[37] and 0.01 M $CaCl_2$ [38], respectively. The content of As^{III}, As^{V}, DMA, MMA, SO_4^{2-}, Cl^-, CO_3^{2-} and NO_3^- in the soil solution was quantified using high-performance liquid chromatography-inductively coupled plasma mass spectrometry (HPLC-ICP-MS, PerkinElmer NexION 300X) [39]. The Cd, Fe, Mn, Ca and Mg concentrations in the soil solution were determined by ICP-OES (Optima 5300DV; PerkinElmer) [40]. The dissolved organic carbon (DOC) was analyzed using a carbon and nitrogen analyzer (Multi N/C 3100, Analytik Jena, Germany).

2.4. Geochemical modeling

The modeling of microcosm aqueous geochemistry was conducted using Visual MINTEQ3.1. For the geochemical modeling, parameters including temperature, pH, DOC (modeled using NICA-Donnan Model), trace elements, anions and cations were incorporated into the geochemical model. It was assumed that the concentrations of tested elements, namely Fe, Mn, Cd, Ca and Mg, are equivalent to their divalent ionic forms (Fe^{2+}, Mn^{2+}, Cd^{2+}, Ca^{2+} and Mg^{2+}) [33]. Furthermore, several redox couples associated with As and Cd bioavailability were included in the model. These couples comprised HS^-/SO_4^{2-}, Fe^{2+}/Fe^{3+}, Mn^{2+}/Mn^{3+}, NH_4^+/NO_3^- and NO_2^-/NO_3^-, with the equilibrium constants (logKs) determined within the model [41]:

$SO_{4^{2-}} + 9H^+ + 8e \Leftrightarrow HS^- + 4H_2O$	$\log Ks = 33.66$
$Fe^{3+} + e \Leftrightarrow Fe^{2+}$	$logKs = 13.032$
$Mn^{3+} + e \Leftrightarrow Mn^{2+}$	$logKs = 25.35$
$NO_{3^-} + 10H^+ + 8e \Leftrightarrow NH_{4^+} + 3H_2O$	$logKs = 119.077$
$NO_{3^-} + 2H^+ + 2e \Leftrightarrow NO_{2^-} + 4H_2O$	$logKs = 28.57$

2.5. DNA extraction and Illumina Miseq sequencing

Total DNA from 36 soil samples (3 replicates × 4 treatments × 3 time points) was extracted using the Fast DNA SPIN Kit for Soil DNA (MP Bio) following the manufacturer's protocols. The concentration and quality of the extracted DNA were assesed using a NanoDrop One spectrophotometer (Thermo Scientific, Wilmington, NC, USA). Subsequently, the DNA was utilized to amplify and sequence the bacterial 16 S rRNA gene which targeted the variable V3-V4 region (forward primer, 338F-5′-ACT CCT ACG GGA GGC AGC AG-3′; reverse primer 806R-5′-GGA CTA CNV GGG TWT CTA AT-3′). Amplicons were sequenced based on the Illumina Miseq platform of Allwegene Technology Co. Ltd (Beijing, China). An operational taxonomic unit (OTU) table was then constructed using the UPARSE pipeline [42]. Briefly, reads were truncated at 300 bp and quality-filtered using a maximum expected error threshold of 0.5. Following the discarding of replicates and singletons, the remaining reads were clustered into OTUs at a 97 % identity level threshold. This process resulted in a 16 S rRNA OTU table encompassing 36 samples × 2742 OTUs (1758,066 reads). The number of high-quality sequences per sample ranged from 21,479 to 84,722. Lastly, representative sequences for each OTU were selected and taxonomically classified against the RDP 16 S rRNA database [43].

2.6. Bioinformatics analysis of 16S rRNA gene profiling

To standardize sequencing depth for subsequent bacterial community analysis, each sample was rarefied to the smallest sample size (21,479) using *R* software through the GUniFrac package (function: Rarefy). Alpha diversity was assessed using a richness index through the VEGAN packages (function: diversity). Weighted Unifrac distances between treatments were calculated using the GUNIFRAC package in *R* and visualized via principal coordinate analysis (PCoA) with the ggplot2 package, illustrating differences in bacterial community structures across all soil samples. Differences in community structure between treatments were assessed using permutational multivariate analysis of variance (PERMANOVA), performed with VEGAN package in *R* (function: adonis), utilizing 9999 permutations. The relative abundance of each taxonomic group per sample was calculated as the number of sequences assigned to that group divided by the total number of sequences. A Random Forest model was constructed using the *R* package RANDOMFOREST to identify key bacteria species that correlated with As and Cd content. The effect of different treatments on the abundance of individual OTUs was assessed using the DESEQ2 package (function: DESeq), employing negative binomial generalized models. Size shrinkage effects were evaluated in each contrast using the lfcShrink() function. To account for multiple testing, a false discovery rate correction (Benjamini-Hochberg procedure) was applied to adjust *P*-values. Additionally, groups of differentially abundant OTUs exhibiting similar changes were identified through hierarchical clustering (Ward's algorithm) on shrunken log fold changes with the hclust() function [44].

2.7. Metagenome analysis

Twelve soil samples (3 replicates × 4 treatments) were collected on the 40th day of incubation. Shotgun metagenomic sequencing was performed on Illumina Hiseq 2500 platform using a paired-end (PE150) sequencing strategy, yielding an average 10 Gb of data per sample. Raw sequencing data were trimmed, filtered assembled by MEGAHIT. Contigs longer than 300 bp were retained for subsequent gene prediction

and annotation.

The Prodigal program (https://github.com/hyattpd/Prodigal) was used to predict the open reading frames (ORF). ORFs with lengths exceeding 200 bp were translated to generate a non-redundant gene catalog, employing criteria of 95 % sequence identity and 90 % coverage. The longest sequence was used as the representative sequence for each cluster through the CD-HIT program (http://www.bioinformatics.org/cd-hit/). Gene depth and relative abundance were computed using the Bowtie2 program. Subsequently, unigenes were annotated against the non-redundant protein sequence database (Version: 2021.11) of the National Center for Biotechnology Information (NCBI) for taxonomy (e-value $\leq$ 0.0001). Additionally, annotation against the Kyoto Encyclopedia of Genes and Genomes (KEGG) for functional classification (e-value $\leq$ 0.0001) was performed using the DIAMOND program (https://github.com/bbuchfink/diamond).

The contigs assembled from each sample were individually separated into bins using the Vamb program (https://github.com/RasmussenLab/vamb). The quality assessment of these bins was conducted utilizing the ChekM program. Bins meeting the criteria of an estimated genome completeness 70 % and contamination below 5 % were retained as high-quality metagenome-assembled genomes (MAGs). Ultimately, 40 high-quality MAGs were obtained for subsequent analysis. The abundance of each MAG across samples was determined as fragments per kilobase of exon per million reads mapped (FPKM) using Salmon. Functional genes within individual MAGs were predicted using Prodigal and annotated against the KEGG database using DIAMOND (with an e-value threshold of $\leq$ 0.0001). Taxonomic classification of all MAGs was performed using GTDB-Tk's classify_wf module.

2.8. Statistical analysis

All statistical analyses were conducted using *R* software (version 3.6.0). Statistical significance was defined as $P < 0.05$ for all tests performed in this study. Unpaired t-tests and two-way analysis of variance (ANOVA) were utilized to assess significant differences. Spearman's rank correlation coefficients between ions and relative abundance of OTUs and As and Cd content were calculated using *R*. *P* value adjustments for multiple comparisons were implemented using false discovery rate (FDR) correction [45]. Heatmap analysis was conducted using the pheatmap package in *R* (function: pheatmap). Partial least squares structural equation modeling (PLS-SEM) was performed using SmartPLS4.0 software [46]. Data plotting was carried out using Prism 9.1.1(GraphPad Software, San Diego, CA, USA) and the 'ggplot2' package in *R*.

3. Results

3.1. Geochemical properties of the incubated soils

The average soil bioavailable As content was 3.34 ± 0.06 mg·kg^{-1} in CK at the conclusion of the incubation period (Fig. 1A). This value significantly decreased ($P < 0.05$) by 27.8 %, 26.3 % and 31.2 % in treatments R, RB and RF, respectively. The concentrations of iAs and DMA in the soil solution exhibited similar trends, with significantly lower concentrations observed in treatments R, RB and RF compared to CK on day 40 (Fig. 1B, Fig. S2). There were no significant differences observed in the available Cd content in the soil and soil solutions among the different treatments. However, the average soil bioavailable Cd content decreased in the following order: CK>R>RF>RB. Spearman's correlation analysis revealed that, apart from SO_4^{2-} ions, the ions present in the soil solutions of R, RB and RF showed stronger correlations with As and Cd compared to those in CK (Fig. 1C). In addition to the two major environmental factors, pH and Eh, we computed the sum of absolute values of correlation coefficients between all chemical species and As and Cd. The top three ions in each group with the highest correlation with As and Cd were as follows: SO_4^{2-}>DOC>CO_3^{2-} in CK, CO_3^{2-}>Mn^{2+}>SO_4^{2-} in R, NO_3^->Mn^{2+}>CO_3^{2-} in RB, and Mn^{2+}>DOC>NO_3^- in RF.

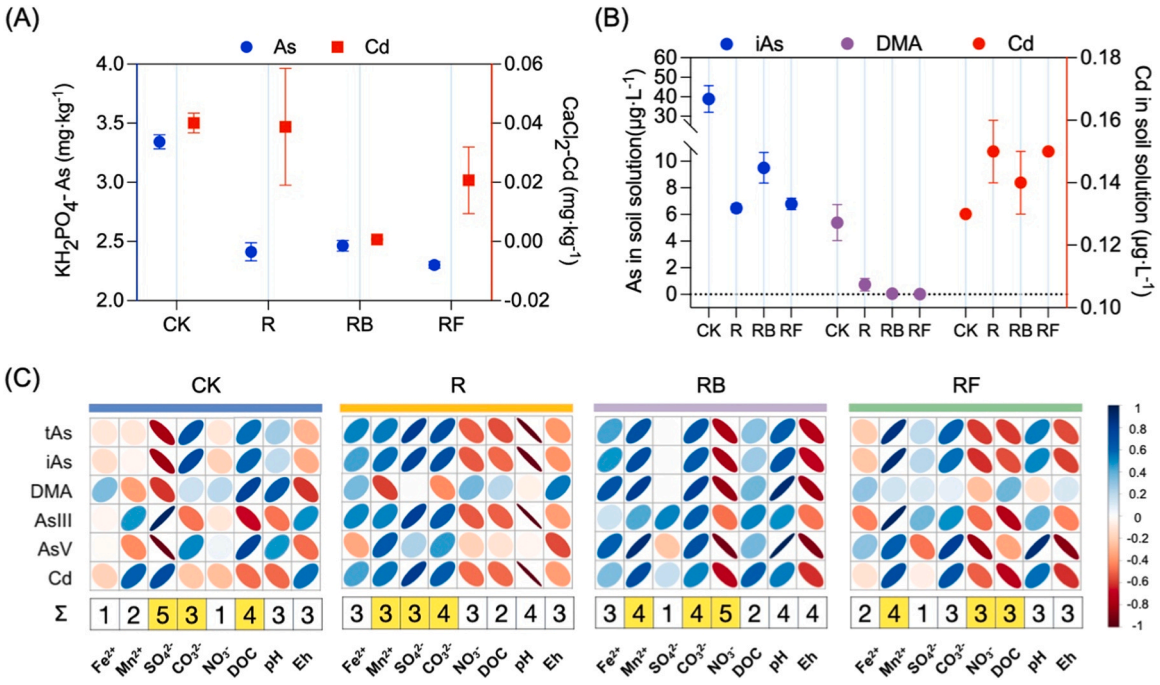

Fig. 1. The available concentrations of As and Cd in soil (A) and the total As and Cd in soil solution (B) on the 40th day. (C) Spearman correlation of As, Cd and ions in soil solution. Data are mean ± standard error (n = 3). $\sum$ represents the sum of the absolute value of the Spearman correlation coefficients in the corresponding column. The top three sum values except those of pH and Eh were highlighted. The area and color of the bubbles represent significant levels. The narrower the bubble, the denser the confidence interval and the stronger the correlation. Red: positive correlation. Blue: negative correlation. CK, flooded paddy soil; R, aerobic paddy soil; RB, biochar application in aerobic paddy soil; RF, application of calcium-magnesium-phosphorus fertilizer in aerobic paddy soil.

3.2. Geochemical modeling

Equilibrium geochemical modeling analysis was employed to investigate the influence of primary redox-active elements on controlling As and Cd concentrations in the soil solution (Fig. 2). The redox speciation of N, Mn, Fe and S is shown in Figs. S3 and S4. The onset of Mn reduction occurs at a redox potential of ~550 mV and lower, whereas N reduction is associated with a redox potential of ~360 mV and lower. The initiation of Fe and S reduction is associated with redox potentials of approximately 50 mV or lower and around − 200 mV or lower, respectively. In the soil solution of the CK sample on the first day of incubation (Eh at 44 mV), the concentrations of As and Cd were primarily associated with Fe and Mn redox, rather than S reduction. In the later stages of the incubation, as the Eh further decreased to between − 190 and − 200 mV, the occurrence of S redox and continued redox of Fe led to a significant increase in the concentration of As and a notable decrease in the concentration of Cd in the soil solution. In the soil solutions of treatments R and RF, As and Cd were predominantly associated with Mn and N redox, while in treatment RB, they were primarily related to redox process involving Fe, Mn and N. As the Eh levels increased, surpassing 50 mV, the reduction process of Fe and Mn shifted towards oxidation, resulting in simultaneous decrease in the concentrations of As and Cd in the soil solutions of treatments R, RB and RF. Further elevation of Eh levels, exceeding 360 mV, accompanied by a decrease in pH, led to a slight increase in the concentrations of As and Cd in the soil solutions of treatments R and RF, possibly due to N oxidation processes.

3.3. Abundance of functional genes involved in multi-element cycles

To better elucidate how microbial community functions impact the biochemical turnover of key ions, we conducted a focused investigation on various genes involved in element cycles, such as Fe, Mn, S and N (Fig. 3 and Fig. S5). Here we found significant differences ($P < 0.05$) in the abundance of functional genes within KEGG and eggNOG L2 pathways across different treatments. Moreover, we observed distinct modules between treatments RB and RF (Fig. S6 and S7). Specifically, regarding the N cycle, CK exhibited a significantly higher abundance of *nifH/nifD/nifK* genes associated with N-fixation for ammonia-related metabolic pathways. Conversly, the relative abundance of *amoA* and *amoB* genes involved in ammonia-oxidation was significantly increased in the RF treatment. The relative abundance of the dissimilatory N reduction gene *napA* was significantly greater in the CK treatment, whereas the relative abundance of assimilatory N reduction genes *nasA, nirA/B*, *narB* was significantly higher in the R treatment. In general, it appeared that RF was associated with an increase in ammonia-oxidizing genes and a decrease in nitrate reduction to ammonium (Fig. 3A). For Mn, the *mntC* gene, encoding the substrate-binding protein of the Mn transport system, was significantly enriched in the RB treatment. Similar trends were observed in the functional genes *mntD*, *troC* and *troD*, which encode permease protein of the Mn transport system. Regarding the Fe and S cycles, we found that genes related to the Fe transport system exhibited higher abundances in RB and RF treatments compared to the R treatment (Fig. S5). However, genes involved in dissimilatory and assimilatory sulfate reduction were significantly more abundant in CK than in other treatments, such as *dsrA* encoding the sulfite reductase α subunit and *dsrB* encoding sulfite reductase β subunit (Fig. S5).

Further statistical analysis showed that PLS-SEM elucidated 76 % and 61 % of the total variation in soil Cd and tAs contents, respectively (Fig. 3C). It was observed that pH and Eh exerted effects on the abundance of functional genes and elemental redox processes. Furthermore, genes associated with Mn and N metabolism were found to influence soil Cd and tAs levels by modulating Mn and N redox states (path coefficient = −0.91 and 0.89, $P < 0.05$). These results suggest that microbial-driven redox transformation of Mn and N play a pivotal role in regulating Cd and tAs content in contaminated soils.

3.4. Bacterial community diversity and composition variation

To elucidate how shifts in microbial diversity and composition correspond to functional changes, we conducted sequencing of the bacterial 16 S rRNA gene across all samples. Overall, a significantly higher bacterial richness index was observed in the RF treatment compared to the R and RB treatments (ANOVA, $P < 0.05$, Fig. 4A). Principal coordinate analysis (PCoA) revealed significant differences in bacterial community structure among CK, R, RB and RF soil samples at 1, 20 and 40 days (PERMANOVA, $P < 0.001$, Fig. 4B). The PCoA plot illustrated distinct clustering of bacterial communities from different time points along the first component (PCoA1), while the separation of CK soil communities from those of R, RB, and RF soils was evident along the second component (PCoA2). The bacterial community composition results were consistent with the findings from PCoA analysis. On day 40, a greater relative abundance of Saccharibacteria and Acidobacteria was evident in the R soil compared to the CK soil. Moreover, relative to other treatments, the RB treatment significantly elevated the relative abundance of Bacteroidetes, while the RF treatment significantly increased the relative abundance of Proteobacteria (Fig. S8).

To identify the main microbial predictors of low Cd and As contents, the abundance of individual OTUs was fitted to negative binomial models and pairwise compared to Wald tests' contrasting control and treatment at each timepoint. A total of 1382 OTUs were affected by treatments at least at one timepoint ($P_{FDR} < 0.05$). After discarding low-abundance OTUs with relative abundance < 0.01 % in all soil samples, random forest models and Spearman's correlation analysis showed that 20 OTUs and 24 OTUs were negatively correlated with Cd and As content, respectively (Fig. 5A). Bradyrhizobiaceae, Sphingomonadaceae, Caulobacteraceae, Comamonadaceae and Thiobacillaceae were the top five families in terms of relative abundance (Fig. 5B). Caulobacteraceae

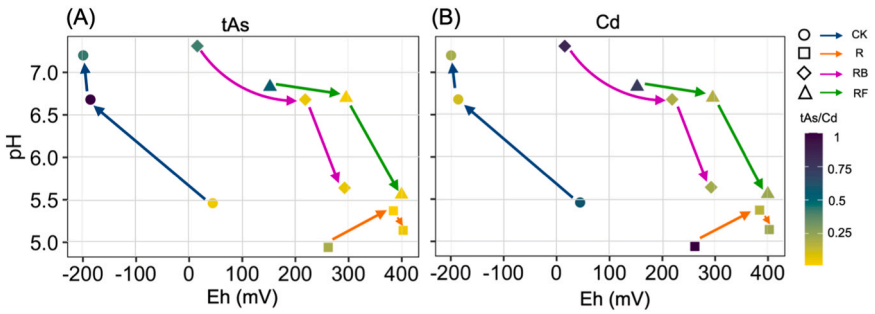

Fig. 2. The ratio of the measured content to the maximum content of dissolved total As (A) and Cd (B) plotted as a function of Eh and pH. The three points in each treatment sequentially connected by arrows are samples on day 1, 20, and 40, respectively. The tAs/Cd content indicated by the color bar was calculated as the ratio of the measured content to the maximum content of As or Cd. CK, flooded paddy soil; R, aerobic paddy soil; RB, biochar application in aerobic paddy soil; RF, application of calcium-magnesium-phosphorus fertilizer in aerobic paddy soil.

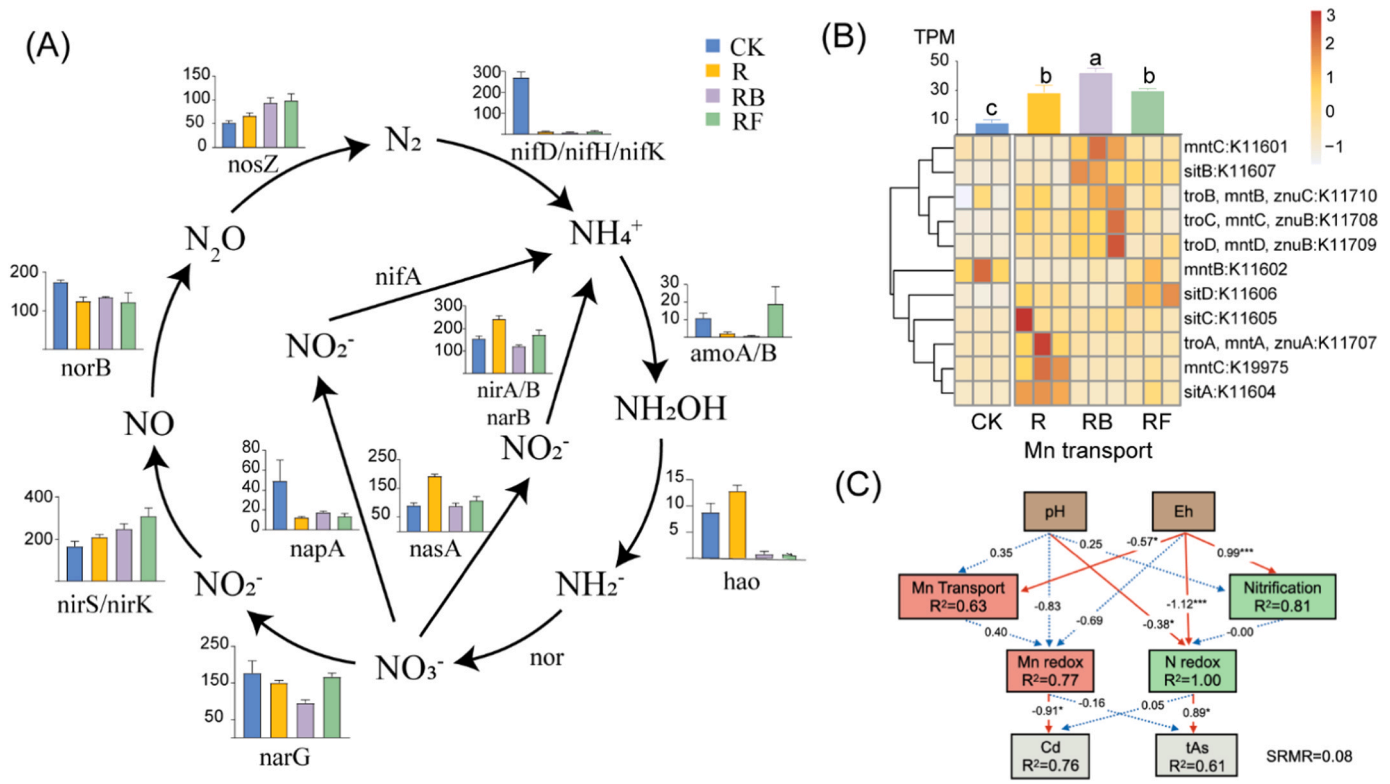

Fig. 3. Differences in the relative abundance (transcripts per kilobase million) of functional genes related to (A) N cycling, (B) Mn cycling and (C) the PLS-SEM model of linkage between crucial genes and Cd and tAs content in soil. CK, flooded paddy soil; R, aerobic paddy soil; RB, biochar application in aerobic paddy soil; RF, application of calcium-magnesium-phosphorus fertilizer in aerobic paddy soil.

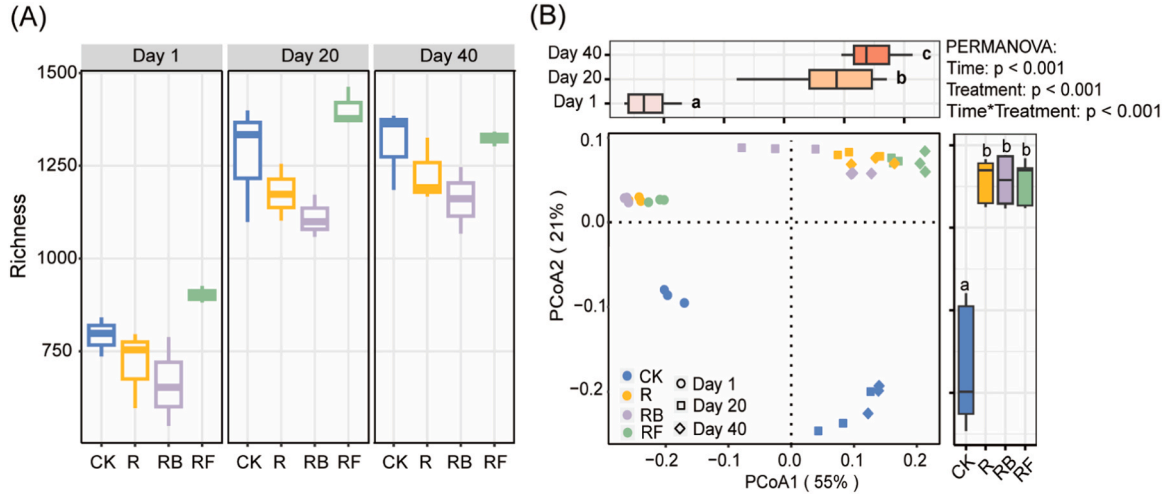

Fig. 4. (A) Bacterial richness among all soil samples (mean ± standard error). (B) Principal coordinate analysis (PCoA) ordinations of bacterial community composition based on Weighted UniFrac distance metric. CK, flooded paddy soil; R, aerobic paddy soil; RB, biochar application in aerobic paddy soil; RF, application of calcium-magnesium-phosphorus fertilizer in aerobic paddy soil.

and Comamonadaceae were mainly enriched in RB treatment soils, while Bradyrhizobiaceae, Sphingomonadaceae, Thiobacillaceae and Chitinophagaceae were primarily enriched in RF treatment soils.

Hierarchical clustering of log_2-fold changes computed across all groups was conducted to further identify coherent patterns of differentially abundant OTUs in soils. Ten clusters were distinguished to illustrate the contrasting trends between treatments (Fig. S9). We observed that 'Cluster 1′ emerged as the most significant cluster for predicting both As and Cd content in soils. 'Cluster 1′ comprised 98 OTUs, with their total relative abundance significantly increasing from day 1 to day 40 in RF treatment soils. This suggests that OTUs enriched in RF treatment soils served as more significant predictors.

3.5. *Functional genes annotation of high-quality MAGs*

We assembled and binned 40 high-quality MAGs (integrity > 10 % and contamination < 5 %) spanning 10 phyla. Consistent with the community composition revealed by 16 S rRNA gene sequencing, over half of these MAGs were affiliated with the dominant bacterial phyla Proteobacteria, Acidobacteriota and archaeal phyla Thermoproteota.

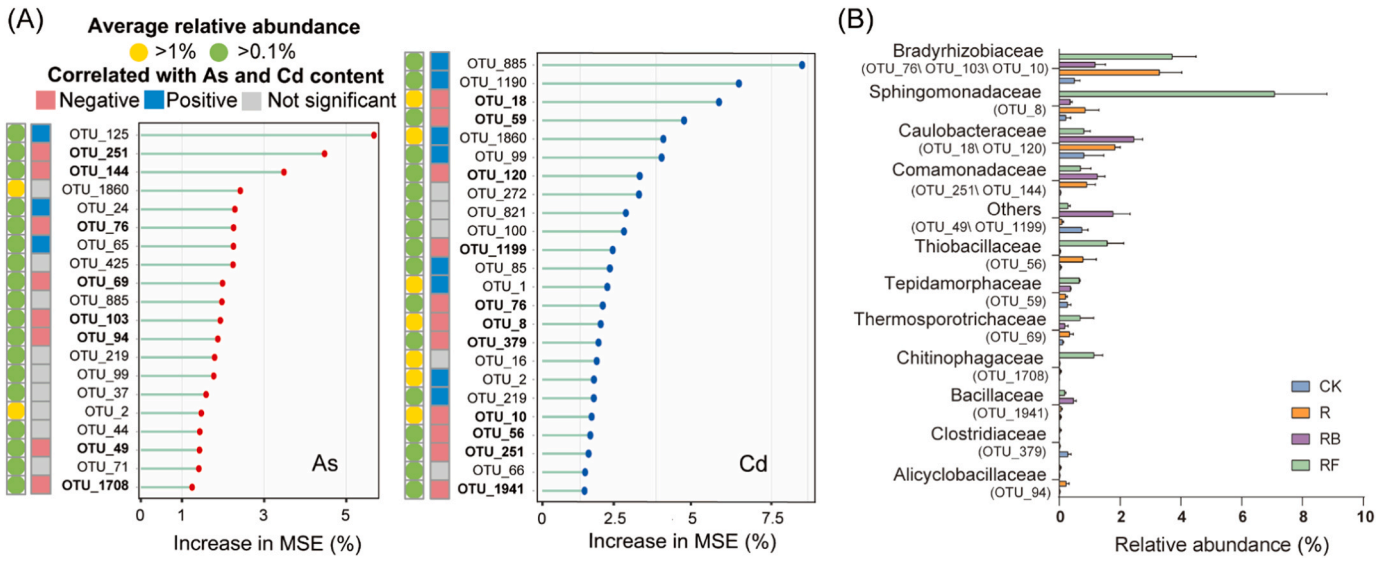

Fig. 5. (A) Random forest mean predictor importance (percentage of increase in mean square error) of the model selection of abundant operational taxonomic units (OTUs) as drivers for the As and Cd content in soil. Percentage increases in the mean squared error (MSE) of variables were used to estimate the importance of these predictors, and higher MSE% values imply more important predictors. Color circles represent the relative abundance of OTUs and color squares show the spearman correlation between OTU abundance and As and Cd content in soil. (B) Bar plot showed the relative abundance of main microbial predictors in different treatments. CK, flooded paddy soil; R, aerobic paddy soil; RB, biochar application in aerobic paddy soil; RF, application of calcium-magnesium-phosphorus fertilizer in aerobic paddy soil.

Functional annotation confirmed their versatile potential for multi-element cycling (Fig. 6). Specifically, the majority of MAGs harbored functional genes involved in nitrate reduction (67.5 %), denitrification (72.5 %), nitrification (27.5 %), sulfate reduction (92.5 %), thiosulfate oxidation (70 %), Mn transport (77.5 %) and Fe transport (100 %). We further investigated the functional genes of representative MAGs belonging to the Bradyrhizobiaceae and Chitinophagaceae families, identified as microbial predictors in the RF treatment. Bradyrhizobiaceae exhibited a higher abundance of Mn and Fe^{III} transport genes, while Chitinophagaceae harbored more genes involved in denitrification. Two MAGs belonging to Caulobacteraceae were enriched in RB soils and carried diverse Fe transport genes. Additionally, four MAGs belonging to Nitrososphaeraceae were predominantly enriched in RF soils, indicating a potential role of archaea in soil nitrification.

4. Discussion

Flooding and drainage, as well as applying chemical or organic fertilizers, are two of most common water management and fertilizer application practices in rice cultivation. The dynamic trends of soil pH

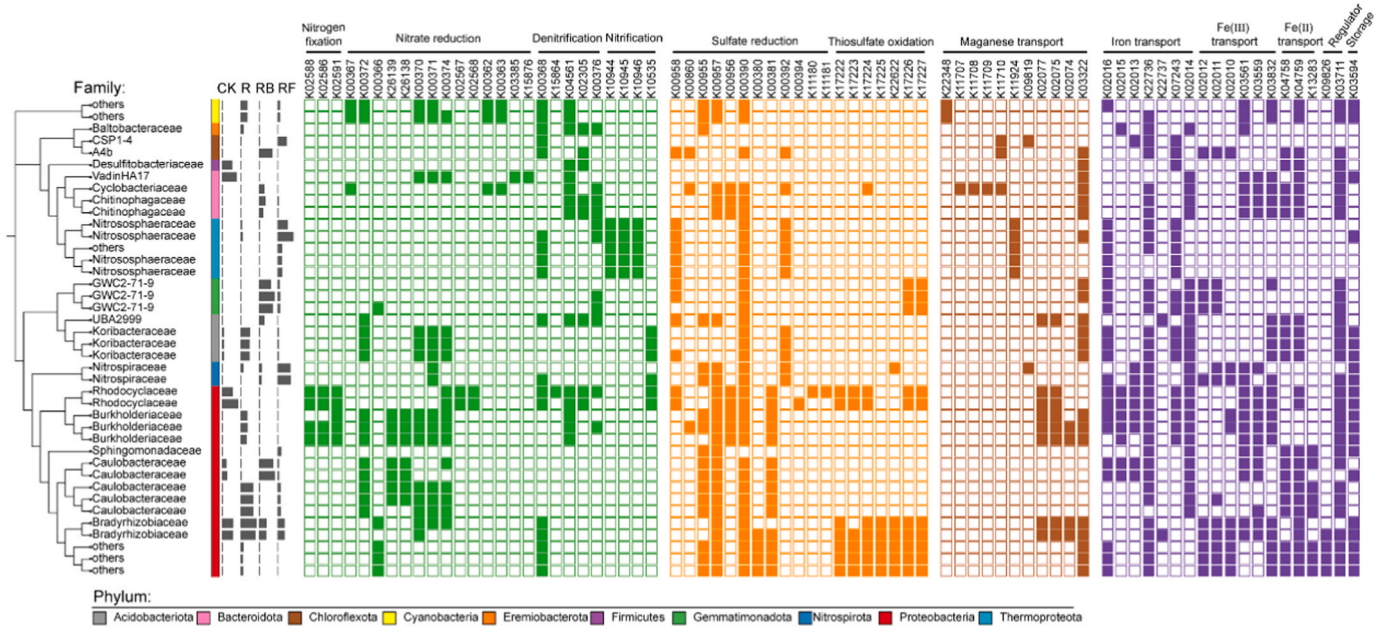

Fig. 6. Phylogenetic and functional characterization of 40 high-quality MAGs. The construction of the maximum likelihood tree was based on a concatenated alignment of 40 marker genes from GTDB-Tk. The bar plot showed the relative abundance of each MAG at four different treatments. The presence (colored) and absence (blank) of protein-encoding genes are represented by the heatmap. CK, flooded paddy soil; R, aerobic paddy soil; RB, biochar application in aerobic paddy soil; RF, application of calcium-magnesium-phosphorus fertilizer in aerobic paddy soil.

and Eh were observed to be completely opposite when the soil was flooded or in aerobic conditions, regardless of whether fertilizers were applied. Currently, computer-based speciation models are widely utilized for predicting metal element speciation in soil or water. Those models offer lower data requirements and time costs compared to traditional analysis methods [47]. In this study, the Cd and As content in contaminated soil and soil solution was successfully reduced by mediating the predominant redox microbial processes of these elements under different conditions. Targeted enhancement of key redox cycles and their corresponding functional microbial activities may be crucial for synergistically reducing the bioavailability of Cd and As.

Under flooded conditions, the As content in the soil solution increased, while the Cd content decreased, consistent with findings demonstrating a gradual decline in soil Eh due to increased irrigation in rice fields [48]. Our investigation revealed that the predominant redox processes in the soil solution were associated with the Fe and S cycles, resulting in elevated concentrations of HS^- and Fe^{2+} in the soil solution under flooded conditions. These may be the two main factors contribute to the dissolution of As and Cd. Specifically, arsenic was mobilized through the reductive dissolution of Fe-(hydro) oxides [13]. As the Eh decreased to approximately − 200 mV, the S redox was initiated. Our findings indicated enhanced expression of *aprA/B* and *dsrA/B* genes encoding the dissimilatory sulfate reduction pathway under these conditions. In the cytoplasm, dissimilatory sulfite reductase (DsrAB) is a key protein in microbial sulfate reduction, which is generally used as a functional marker for this process in the environmental and genomic studies [49]. Enriched sulfate reducing bacteria (SRB) in paddy fields [50] likely play a crucial role in the generation of $S^{2-}$and HS^- ions [51]. This process is implicated in the formation of CdS, which typically leads to a reduction in Cd availability. Additionally, the concurrent presence of Fe^{2+} ions could facilitate co-precipitate with As^{III} in the presence of FeS [16]. This phenomenon might account for the reduction in As concentration observed in the soil solution following a decrease in Eh to − 200 mV. In our study area, fertilizers are typically applied to paddy fields after drainage to maximize their effectiveness. Although we did not apply biochar or calcium-magnesium-phosphate fertilizers under flooded conditions, previous studies in similar acidic paddy fields have shown that biochar application delays the decline of Eh and inhibits reduction reactions under flooding [52]. The application of calcium-magnesium-phosphate fertilizers had little to no effect on Eh [53]. Over time, the redox states of these treatments were similar to those observed in fields subjected to flooding alone.

In contrast, under aerobic conditions in paddy fields, Fe, Mn and N redox cycling were dominant. As Eh increases, the oxidation of soluble Fe^{2+} led to a decrease in its aqueous concentration; however, this reduction does not fully explain the increase in Fe^{3+} content in the soil solution. We hypothesize that Fe^{2+} was oxidized to form solid Fe-(hydr) oxides, which subsequently adsorb As. Our previous findings support this hypothesis, suggesting that the increased As content associated with Fe oxides may be attributable to this process [24]. Since the highest value of the Eh range in this study remained lower than the onset of Mn oxidation in the geochemical model, dissolved Mn predominantly existed in the form of Mn^{2+}. Nevertheless, the content of Mn^{3+} increased after reoxygenation compared to flooding conditions. Prior studies have demonstrated that heterovalent Mn minerals in mixed valence states will be formed in the oxidation state, which exhibit strong adsorption affinity for metal ions such as dissolved As and Cd [54]. Mn oxides production in the environment is believed to be predominately driven by biological activity, as microorganisms oxidize Mn^{II} at kinetically faster rates than many abiotic reactions [55]. Due to the dearth of research on intracellular Mn oxidation in microorganisms, we were unable to annotate specific Mn oxidation genes. However, operative Mn transport system always expression in Mn^{II}-oxidizing bacterial [56]. The presence of enriched *mntC*, *sitaA/B/C* and *troA/B/C/D* genes in the aerobic soil suggests their potential contribution to the Mn uptake pathway, hinting at microbial involvement in the Mn oxidation process [57].

Here, we found that the potential functional taxa of Bradyrhizobiaceae family accumulated in low As and Cd content soils may carry multiple Mn and Fe^{III} transport genes. Recent studies have also reported a relatively high abundance of bacteria within the Bradyrhizobiaceae family, suggesting a potential association with Mn-oxidizing bacteria [58]. Observations indicate that when the Eh reaches approximately 400 mV and the pH decreases to 5.5 and lower, N oxidizes. However, this dynamic N reaction leads to the generation of a large amount of H^+, which compete with Cd^{2+} ions for adsorption sites, potentially resulting in increased availability of Cd. Conversely, As tends to be adsorbed by the soil, consequently reducing its content in the soil solution.

Varied soil ecological functions are always provided by different taxonomic compositions [25]. Applying biochar or calcium-magnesium-phosphate fertilizers in aerobic soil can improve soil nutrients levels and influence the soil microbial structure, affecting both bacterial alpha diversity and beta diversity. Interestingly, RF and RB showed significantly different microbial richness. Chemical fertilizers can rapidly increase the content of available nutrients in the soil, thereby enhancing the diversity of microbial communities in a short period. However, the difference in microbial diversity between RB and RF decreases over time. The decomposition of nutrients in organic matter requires more time to be released [59]. These alternations subsequently influence the redox cycles of Fe, Mn and N, resulting in both beneficial and detrimental outcomes. The contents of both Fe^{2+} and Fe^{3+} in the soil solution were observed to be lower compared to the non-fertilized drained treatment, potentially indicating an intensified process of Fe oxidation leading to the formation of solid minerals.

Moreover, the distinct physicochemical properties of inorganic and organic fertilizers themselves also play a role in shaping these processes. After applying biochar, Eh did not reach the onset of N oxidation, but the N-related processes were observed, potentially attributed to the biochar addition simulating the activity of relevant microorganisms. There is a feedback mechanism between Cd and soil nitrification: H^+ ions with a larger hydrated ion radius, produced by nitrification, desorb Cd^{2+} from soil particles, increasing its mobility. Conversely, Cd inhibits the nitrification process and proton (H^+) production by poisoning the growth of AOA and AOB communities, thereby inhibiting its own migration. After applying biochar, the reduction of Cd toxicity and improvement in soil conditions accelerate the recovery of AOA and AOB and nitrification due to biochar's adsorption effect. However, due to the slow calcification of biochar, the enhanced nitrification will not induce acidification [60]. However, these processes exhibited lower activity compared to R or RF treatments. Moreover, the higher pH observed in RB treatments may result in elevated iAs levels in the soil solution [12]. In addition, applying biochar as an organic amendment increased the content of DMA, known for its high toxicity to rice, potentially contributing to the occurrence of rice straight head disease.

After applying calcium magnesium phosphate fertilizer, the ammonia-oxidizing genes (*amoA/amoB*) were significantly more abundant, potentially attributed to the presence of CaO and MgO in the inorganic fertilizer. After liming, significant alterations were observed in the AOA and AOB communities in the field, subsequently impacting gross nitrification activity [20]. Notably, the representative MAGs affiliated with Nitrososphaeraceae (AOA) and Nitrospiraceae (AOB) were identified in the RF treatment, suggesting that the related nitrification gene-carrying microorganisms are active under this condition [61,62]. The NH_4^+ input and aeration can also facilitate nitrification [63]. The liming effect of CMP neutralizes soil acidification, thereby reducing the risk of increased available Cd. Although phosphorus fertilizer may be an important factor affecting the bioavailability of Cd and As, we did not detect PO_4^{3-} in the soil solution samples using HPLC-ICP-MS. Therefore, we speculate that phosphorus plays a very small role in the element redox cycle in the soil solution and is more likely to play a role in fixing Cd by forming cadmium phosphate precipitates [64]. The increase in Mn^{3+} content may be attributed to enhanced oxidation processes, which led to the amplification of the

impact of Mn in RB treatment. Our results highlight the important role of biogeochemical cycles in reducing As and Cd availability. While the role of microorganisms should not be overestimated, our finding suggest that the bioremediation should be taken into account in future research and global sustainable development goals.

5. Conclusion

In this study, we explored the effects of water regime and the application of both organic and inorganic fertilizers on As and Cd co-contaminated environments, highlighting the importance of the redox cycles chain and microbial ecological functions in mitigating the As and Cd bioavailability. Geochemical modeling and shotgun metagenomic analyses showed that the redox chain was primarily composed of Fe and S cycles under flooding. These cycles played a role in elevating As risk and decreasing Cd risk. Conversely, under aerobic conditions, the redox chain was predominantly driven by the "cogs" representing Fe, Mn and N redox processes. The oxidation of Fe and Mn minerals facilitated the adsorption of Cd and As, thereby reducing their contents in the soil solution. However, the intensified N cycle resulted in soil acidification, increasing the risk of Cd but further decreasing As contents. Despite the promotion of nitrification with the application of CMP fertilizer, the liming effect induced by CMP mitigated the risk of Cd associated by soil acidification. While the application of biochar led to the amplification of the impact of Mn and effectively delayed N oxidation, which typically requires a higher Eh onset. Results of 16 S rRNA gene sequencing further revealed that diverse field water management and fertilization practices differently influence microbial diversity, composition, and the abundance of key species harboring functional genes, thereby initiating various elemental cycle reactions.

Utilization of CMP fertilizer or organic fertilizer in aerobic rice cultivation not only ensures optimal yield but also enhances essential elements cycling, synergistically reducing the bioavailability of Cd and As. In addition, biochar exhibits environmentally friendliness characteristics and contribute to carbon sequestration, rendering it a promising material. Future field trials across diverse soil types and climatic conditions are warranted to ascertain broader applicability.

Funding

This work was financially supported by the National Foundation of Natural Science of China, Grant No. 42077139; the China Postdoctoral Science Foundation (2023M743823); the Science Innovation Project of the Chinese Academy of Agricultural Science (CAAS-ASTIP-2021-IEDA); and the special fund for Science and Technology Innovation Teams of Shanxi Province (202304051001016).

CRediT authorship contribution statement

Shiming Su: Writing – review & editing, Validation, Supervision, Project administration, Methodology, Funding acquisition, Conceptualization. **Xibai Zeng:** Writing – review & editing, Supervision, Project administration. **Hong Shan:** Writing – review & editing, Investigation. **Sanjai J. Parikh:** Writing – review & editing. **Yifei Sun:** Writing – original draft, Visualization, Validation, Software, Methodology, Investigation, Funding acquisition, Data curation. **Ting Zhang:** Writing – original draft, Visualization, Software, Methodology, Investigation, Formal analysis, Data curation. **Nan Zhang:** Writing – review & editing. **Lijuan Huo:** Writing – review & editing, Funding acquisition. **Gina Garland:** Writing – review & editing. **Gilles Colinet:** Writing – review & editing.

Declaration of Competing Interest

The authors declare that they have no known competing financial interests or personal relationships that could have appeared to influence the work reported in this paper.

Data availability

Data will be made available on request.

Appendix A. Supporting information

Supplementary data associated with this article can be found in the online version at doi:10.1016/j.jhazmat.2024.135244.

References

[1] Khan, S., Naushad, M., Lima, E.C., Zhang, S., Shaheen, S.M., Rinklebe, J., 2021. Global soil pollution by toxic elements: Current status and future perspectives on the risk assessment and remediation strategies–a review. J Hazard Mater 417, 126039.
[2] National Toxicology Program (NTP). 2000. Tenth Report on Carcinogens. Department of Health and Human Services, Research Triangle Park, III-42–III-44.
[3] International Agency for Research on Cancer (IARC). 2009. IARC Monographs on the identification of carcinogenic hazards to humans. <⟨https://monographs.iarc.who.int/list-of-classifications⟩>.
[4] Zhao, D., Wang, P., Zhao, F.J., 2023. Dietary cadmium exposure, risks to human health and mitigation strategies. Crit Rev Environ Sci Technol 53 (8), 939–963.
[5] Smith, A.H., Lingas, E.O., Rahman, M., 2000. Contamination of drinking-water by arsenic in Bangladesh: a public health emergency. Bull World Health Organ 78 (9), 1093–1103.
[6] Liu, T., Lawluvy, Y., Shi, Y., Ighalo, J.O., He, Y., Zhang, Y., et al., 2022. Adsorption of cadmium and lead from aqueous solution using modified biochar: a review. J Environ Chem Eng 10 (1), 106502.
[7] Zhao, F.J., Zhu, Y.G., Meharg, A.A., 2013. Methylated arsenic species in rice: geographical variation, origin, and uptake mechanisms. Environ Sci Technol 47 (9), 3957–3966.
[8] Zheng, M.Z., Li, G., Sun, G.X., Shim, H., Cai, C., 2013. Differential toxicity and accumulation of inorganic and methylated arsenic in rice. Plant Soil 365, 227–238.
[9] Honma, T., Ohba, H., Kaneko-Kadokura, A., Makino, T., Nakamura, K., Katou, H., 2016. Optimal soil Eh, pH, and water management for simultaneously minimizing arsenic and cadmium concentrations in rice grains. Environ Sci Technol 50 (8), 4178–4185.
[10] Afzal, M., Yu, M., Tang, C., Zhang, L., Muhammad, N., Zhao, H., et al., 2019. The negative impact of cadmium on nitrogen transformation processes in a paddy soil is greater under non-flooding than flooding conditions. Environ Int 129, 451–460.
[11] Yin, Y., Wang, Y., Ding, C., Zhou, Z., Tang, X., He, L., et al., 2024. Impact of iron and sulfur cycling on the bioavailability of cadmium and arsenic in co-contaminated paddy soil. J Hazard Mater 465, 133408.
[12] Jiku, M.A.S., Zeng, X., Li, L., Li, L., Zhang, Y., Huo, L., et al., 2022. Soil ridge cultivation maintains grain As and Cd at low levels and inhibits As methylation by changing arsM-harboring bacterial communities in paddy soils. J Hazard Mater 429, 128325.
[13] Suda, A., Makino, T., 2016. Functional effects of manganese and iron oxides on the dynamics of trace elements in soils with a special focus on arsenic and cadmium: a review. Geoderma 270, 68–75.
[14] Wang, Z., Liu, X., Liang, X., Dai, L., Li, Z., Liu, R., et al., 2022. Flooding-drainage regulate the availability and mobility process of Fe, Mn, Cd, and As at paddy soil. Sci Total Environ 817, 152898.
[15] Huang, H., Chen, H.P., Kopittke, P.M., Kretzschmar, R., Zhao, F.J., Wang, P., 2021. The voltaic effect as a novel mechanism controlling the remobilization of cadmium in paddy soils during drainage. Environ Sci Technol 55 (3), 1750–1758.
[16] Roy, M., Giri, A.K., Dutta, S., Mukherjee, P., 2015. Integrated phytobial remediation for sustainable management of arsenic in soil and water. Environ Int 75, 180–198.
[17] Chen, C., Li, L., Huang, K., Zhang, J., Xie, W.Y., Lu, Y., et al., 2019. Sulfate-reducing bacteria and methanogens are involved in arsenic methylation and demethylation in paddy soils. ISME J 13 (10), 2523–2535.
[18] Ninin, J.M.L., Muehe, E.M., Kölbl, A., Mori, A.H., Nicol, A., Gilfedder, B., et al., 2024. Changes in arsenic mobility and speciation across a 2000-year-old paddy soil chronosequence. Sci Total Environ 908, 168351.
[19] Zhang, M., Kolton, M., Häggblom, M.M., Sun, X., Yu, K., He, B., et al., 2022. Anaerobic ammonium oxidation coupled to arsenate reduction, a novel biogeochemical process observed in arsenic-contaminated paddy soil. Geochim Et Cosmochim Acta 335, 11–22.
[20] Zhang, M.M., Alves, R.J., Zhang, D.D., Han, L.L., He, J.Z., Zhang, L.M., 2017. Time-dependent shifts in populations and activity of bacterial and archaeal ammonia oxidizers in response to liming in acidic soils. Soil Biol Biochem 112, 77–89.
[21] Wang, C., Huang, Y., Zhang, C., Zhang, Y., Yuan, K., Xue, W., et al., 2021. Inhibition effects of long-term calcium-magnesia phosphate fertilizer application on Cd uptake in rice: Regulation of the iron-nitrogen coupling cycle driven by the soil microbial community. J Hazard Mater 416, 125916.
[22] Yang, Y., Rao, X., Zhang, X., Liu, M., Fu, Q., Zhu, J., et al., 2021. Effect of P/As molar ratio in soil porewater on competitive uptake of As and P in As sensitive and tolerant rice genotypes. Sci Total Environ 797, 149185.

[23] Zhao, F.J., Wang, P., 2020. Arsenic and cadmium accumulation in rice and mitigation strategies. Plant Soil 446, 1–21.
[24] Zhang, T., Jiku, M.A.S., Li, L., Ren, Y., Li, L., Zeng, X., et al., 2023. Soil ridging combined with biochar or calcium-magnesium-phosphorus fertilizer application: Enhanced interaction with Ca, Fe and Mn in new soil habitat reduces uptake of as and Cd in rice. Environ Pollut, 121968.
[25] Zhang, L.Z., Xing, S.P., Huang, F.Y., Xiu, W., Rensing, C., Zhao, Y., et al., 2024. Metabolic coupling of arsenic, carbon, nitrogen, and sulfur in high arsenic geothermal groundwater: Evidence from molecular mechanisms to community ecology. Water Res 249, 120953.
[26] Aryal, B., Gurung, R., Camargo, A.F., Fongaro, G., Treichel, H., Mainali, B., et al., 2022. Nitrous oxide emission in altered nitrogen cycle and implications for climate change. Environ Pollut, 120272.
[27] Schaeffer, S.M., Homyak, P.M., Boot, C.M., Roux-Michollet, D., Schimel, J.P., 2017. Soil carbon and nitrogen dynamics throughout the summer drought in a California annual grassland. Soil Biol Biochem 115, 54–62.
[28] Han, L., Qin, H., Wang, J., Yao, D., Zhang, L., Guo, J., et al., 2023. Immediate response of paddy soil microbial community and structure to moisture changes and nitrogen fertilizer application. Front Microbiol 14, 1130298.
[29] Weitao, L.I., Meng, W.U., Ming, L.I.U., Jiang, C., Xiaofen, C.H.E.N., Kuzyakov, Y., et al., 2018. Responses of soil enzyme activities and microbial community composition to moisture regimes in paddy soils under long-term fertilization practices. Pedosphere 28 (2), 323–331.
[30] Liu, H., Qin, S., Li, Y., Zhao, P., Nie, Z., Liu, H., 2023. Comammox Nitrospira and AOB communities are more sensitive than AOA community to different fertilization strategies in a fluvo-aquic soil. Agric, Ecosyst Environ 342, 108224.
[31] Mohapatra, M., Yadav, R., Rajput, V., Dharne, M.S., Rastogi, G., 2021. Metagenomic analysis reveals genetic insights on biogeochemical cycling, xenobiotic degradation, and stress resistance in mudflat microbiome. J Environ Manag 292, 112738.
[32] Chen, C., Shen, Y., Li, Y., Zhang, W., Zhao, F.J., 2021. Demethylation of the antibiotic methylarsenite is coupled to denitrification in anoxic paddy soil. Environ Sci Technol 55 (22), 15484–15494.
[33] Maguffin, S.C., Abu-Ali, L., Tappero, R.V., Pena, J., Rohila, J.S., McClung, A.M., et al., 2020. Influence of manganese abundances on iron and arsenic solubility in rice paddy soils. Geochim Et Cosmochim Acta 276, 50–69.
[34] Xue, S., Jiang, X., Wu, C., Hartley, W., Qian, Z., Luo, X., et al., 2020. Microbial driven iron reduction affects arsenic transformation and transportation in soil-rice system. Environ Pollut 260, 114010.
[35] Shi, S., Wu, Q., Zhu, Y., Fan, Z., Rensing, C., Liu, H., et al., 2022. Risk assessment of using phosphate and calcium fertilisers for continuously flooded rice cultivation in a soil co-contaminated with cadmium and antimony. Crop Pasture Sci 73 (5), 585–598.
[36] ur Rehman, M.Z., Khalid, H., Akmal, F., Ali, S., Rizwan, M., Qayyum, M.F., et al., 2017. Effect of limestone, lignite and biochar applied alone and combined on cadmium uptake in wheat and rice under rotation in an effluent irrigated field. Environ Pollut 227, 560–568.
[37] Xu, D.M., Fu, R.B., 2022. Mechanistic insight into the release behavior of arsenic (As) based on its geochemical fractions in the contaminated soils around lead/zinc (Pb/Zn) smelters. J Clean Prod 363, 132348.
[38] Houba, V.J.G., Temminghoff, E.J.M., Gaikhorst, G.A., Van Vark, W., 2000. Soil analysis procedures using 0.01 M calcium chloride as extraction reagent. Commun Soil Sci Plant Anal 31 (9-10), 1299–1396.
[39] Yan, M., Zeng, X., Wang, J., Meharg, A.A., Meharg, C., Tang, X., et al., 2020. Dissolved organic matter differentially influences arsenic methylation and volatilization in paddy soils. J Hazard Mater 388, 121795.
[40] Cruz, S.M., Schmidt, L., Dalla Nora, F.M., Pedrotti, M.F., Bizzi, C.A., Barin, J.S., et al., 2015. Microwave-induced combustion method for the determination of trace and ultratrace element impurities in graphite samples by ICP-OES and ICP-MS. Microchem J 123, 28–32.
[41] Gustafsson, J.P., 2020. Visual MINTEQ (version 3.1). Department of Land and Water Resources Engineering. R Inst Technol: Stockh, Swed.
[42] Edgar, R.C., 2013. UPARSE: highly accurate OTU sequences from microbial amplicon reads. Nat Methods 10 (10), 996–998.
[43] Wang, Q., Garrity, G.M., Tiedje, J.M., Cole, J.R., 2007. Naive Bayesian classifier for rapid assignment of rRNA sequences into the new bacterial taxonomy. Appl Environ Microbiol 73 (16), 5261–5267.
[44] Santos-Medellín, C., Liechty, Z., Edwards, J., Nguyen, B., Huang, B., Weimer, B.C., et al., 2021. Prolonged drought imparts lasting compositional changes to the rice root microbiome. Nat Plants 7 (8), 1065–1077.
[45] Benjamini, Y., Hochberg, Y., 1995. Controlling the false discovery rate: a practical and powerful approach to multiple testing. J R Stat Soc: Ser B (Methodol 57 (1), 289–300.
[46] Ringle, Christian M., Wende, Sven, & Becker, Jan-Michael. (2022). SmartPLS 4. Oststeinbek: SmartPLS. <⟨https://www.smartpls.com⟩>.
[47] Khalid, S., Shahid, M., Alothman, Z.A., Al-Kahtani, A.A., Murtaza, B., Dumat, C., 2023. Predicting chemical speciation of metals in soil using Visual Minteq. Soil Ecol Lett 5 (3), 220162.
[48] Hu, P., Ouyang, Y., Wu, L., Shen, L., Luo, Y., Christie, P., 2015. Effects of water management on arsenic and cadmium speciation and accumulation in an upland rice cultivar. J Environ Sci 27, 225–231.
[49] Neukirchen, S., Pereira, I.A., Sousa, F.L., 2023. Stepwise pathway for early evolutionary assembly of dissimilatory sulfite and sulfate reduction. ISME J 17 (10), 1680–1692.
[50] Wakao, N., Furusaka, C., 1973. Distribution of sulfate-reducing bacteria in paddy-field soil. Soil Sci Plant Nutr 19 (1), 47–52.
[51] Huang, H., Lv, Y., Tian, K., Shen, Y., Zhu, Y., Lu, H., et al., 2023. Influence of sulfate reducing bacteria cultured from the paddy soil on the solubility and redox behavior of Cd in a polymetallic system. Sci Total Environ 901, 166369.
[52] Li, H., Li, Z., Huang, L., Mao, X., Dong, Y., Fu, S., et al., 2023. Environmental factors influence the effects of biochar on the bioavailability of Cd and Pb in soil under flooding condition. Water Air Soil Pollut 234 (2), 100.
[53] Luo, W., Yang, S., Khan, M.A., Ma, J., Xu, W., Li, Y., et al., 2020. Mitigation of Cd accumulation in rice with water management and calcium-magnesium phosphate fertilizer in field environment. Environ Geochem Health 42, 3877–3886.
[54] Wang, X., Xie, G.J., Tian, N., Dang, C.C., Cai, C., Ding, J., et al., 2022. Anaerobic microbial manganese oxidation and reduction: a critical review. Sci Total Environ 822, 153513.
[55] Tebo, B.M., 1991. Manganese (II) oxidation in the suboxic zone of the Black Sea. Deep Sea Res Part A Oceanogr Res Pap 38, S883–S905.
[56] Learman, D.R., Hansel, C.M., 2014. Comparative proteomics of Mn (II)-oxidizing and non-oxidizing R oseobacter clade bacteria reveal an operative manganese transport system but minimal Mn (II)-induced expression of manganese oxidation and antioxidant enzymes. Environ Microbiol Rep 6 (5), 501–509.
[57] Wang, M., Chen, S., Shi, H., Liu, Y., 2022. Redox dependence of manganese controls cadmium isotope fractionation in a paddy soil-rice system under unsteady pe+ pH conditions. Sci Total Environ 806, 150675.
[58] Matsushita, S., Komizo, D., Cao, L.T.T., Aoi, Y., Kindaichi, T., Ozaki, N., et al., 2018. Production of biogenic manganese oxides coupled with methane oxidation in a bioreactor for removing metals from wastewater. Water Res 130, 224–233.
[59] Quan, T.A.N.G., Yongqiu, X.I.A., Chaopu, T.I., Jun, S.H.A.N., Wei, Z.H.O.U., Chenglin, L.I., et al., 2023. Partial organic fertilizer substitution promotes soil multifunctionality by increasing microbial community diversity and complexity. Pedosphere 33 (3), 407–420.
[60] Zhao, H., Yu, L., Yu, M., Afzal, M., Dai, Z., Brookes, P., et al., 2020. Nitrogen combined with biochar changed the feedback mechanism between soil nitrification and Cd availability in an acidic soil. J Hazard Mater 390, 121631.
[61] Liu, J., Guo, Y., Gu, H., Liu, Z., Hu, X., Yu, Z., et al., 2023. Conversion of steppe to cropland increases spatial heterogeneity of soil functional genes. ISME J 17 (11), 1872–1883.
[62] Zhen, Z., Li, G., Chen, Y., Wei, T., Li, H., Huang, F., et al., 2023. Accelerated nitrification and altered community structure of ammonia-oxidizing microorganisms in the saline-alkali tolerant rice rhizosphere of coastal solonchaks. Appl Soil Ecol 189, 104978.
[63] Blaud, A., van der Zaan, B., Menon, M., Lair, G.J., Zhang, D., Huber, P., et al., 2018. The abundance of nitrogen cycle genes and potential greenhouse gas fluxes depends on land use type and little on soil aggregate size. Appl Soil Ecol 125, 1–11.
[64] Matusik, J., Bajda, T., Manecki, M., 2008. Immobilization of aqueous cadmium by addition of phosphates. J Hazard Mater 152 (3), 1332–1339.